Inhibition of histone deacetylase 3 by MiR-494 alleviates neuronal loss and improves neurological recovery in experimental stroke

Haiping Zhao[1,2,3,*], Guangwen Li[1,2,*], Sijia Zhang[1,2],
Fangfang Li[1], Rongliang Wang[1,2], Zhen Tao[1,2], Qingfeng Ma[1],
Ziping Han[1], Feng Yan[1], Junfen Fan[1], Lingzhi Li[1,2],
Xunming Ji[1,2,3] and Yumin Luo[1,2,3] (ID)

Abstract

HDAC3 is an essential negative regulator of neuronal plasticity and memory formation. Although a chemical inhibitor has been invented, little is known about its endogenous modulators. We explored whether miR-494 affects HDAC3-mediated neuronal injury following acute ischemic stroke. A substantial increase in plasma miR-494 was detected in AIS patients and was positively associated with the mRS at one year after symptom onset. The miR-494 levels were transiently increased in the infarcted brain tissue of mice. In contrast, miR-494 levels were reduced in neurons but increased in the medium after OGD. Intracerebroventricular injection of miR-494 agomir reduced neuronal apoptosis and infarct volume at the acute stage of MCAO, promoted axonal plasticity and long-term outcomes at the recovery stage, suppressed neuronal ataxin-3 and HDAC3 expression and increased acetyl-H3K9 levels in the ipsilateral hemisphere. In vitro studies confirmed that miR-494 posttranslationally inhibited HDAC3 in neurons and prevented OGD-induced neuronal axonal injury. The HDAC3 inhibitor increased acetyl-H3K9 levels and reversed miR-494 antagomir-aggravated acute cerebral ischemic injury, as well as brain atrophy and long-term functional recovery. These results suggest that miR-494 may serve as a predictive biomarker of functional outcomes in AIS patients and a potential therapeutic target for the treatment of ischemic stroke.

Introduction

The prevalence of cerebrovascular disease will continue to ascend along with the aging of the global population, and the costs of long-term stroke care are still increasing due to the rising adult disability. The amount of hypoxia-related neuronal death or axon injury leads to neurological function deficits and cognitive impairment. Recently, with the understanding of stroke pathology and the extension of the time window of treatment associated with embolectomy, there has been a resurrection of research on developing neuroprotective agents for stroke treatment. Novel molecular targets and therapies are desperately needed to improve neuronal recovery after ischemic stroke.

[1]Institute of Cerebrovascular Disease Research and Department of Neurology, Xuanwu Hospital of Capital Medical University, Beijing, China
[2]Beijing Geriatric Medical Research Center and Beijing Key Laboratory of Translational Medicine for Cerebrovascular Diseases, Beijing, China
[3]Beijing Institute for Brain Disorders, Capital Medical University, Beijing, China

*These authors contributed equally to this work.

Corresponding author:
Yumin Luo, Institute of Cerebrovascular Diseases Research and Department of Neurology, Xuanwu Hospital of Capital Medical University, 45 Changchun Street, Beijing 100053, China.
Email: yumin111@ccmu.edu.cn

Histone deacetylases (HDACs) have gained great interest over the past few years and are currently being investigated as molecular targets for the pharmacological treatment of stroke for their contributions to neuronal death and plasticity. Research indicates that HDAC3 positively regulates a subset of neuronal genes through Forehead box O (FOXO) deacetylation[1] and negatively regulates memory formation[2] in specific brain regions.[3] Strikingly, the HDAC3 inhibitor RGFP966 has been shown to precondition the brain and evoke endogenous protection against ischemic insults,[4] and intranasal administration of HDAC3 siRNA diminished cognitive impairments in a mouse model of Fragile X syndrome.[5] Moreover, RGFP966 also promotes functional recovery after spinal cord injury by dampening inflammatory cytokines,[6] indicating that RGFP966 may be a potential therapeutic medication combating microglia activation in the central nervous system.[7] Therefore, the discovery of an endogenous HDAC3 suppressor is of great significance.

MicroRNA (miR)-494 was originally proposed to act as a tumor suppressor[8,9] and has been implicated in ischemic disease[10] and neurodegeneration.[11] MiR-494 inhibited neural apoptosis and improved functional recovery by modulating the phosphatase and tensin homolog (PTEN)/AKT/mechanistic target of rapamycin (mTOR) pathway in rats with spinal cord injury.[12] In contrast, miR-494 aggravated oxygen and glucose deprivation (OGD)-induced PC12 cell injury.[13] However, the function and mechanism of miR-494 in neuron injury after cerebral ischemia are unknown. It has been indicated that endogenous miR-494 downregulated ataxin-3 (ATXN3) through interacting with the 3′ UTR of ATXN3,[14] which positively regulates HDAC3 by deubiquitinating and stabilizing HDAC3.[15] Furthermore, an acute ethanol-induced miR-494 reduction in the amygdala was anxiolytic through increased acetyl-H3K9-mediated chromatin remodeling.[16] The above clues led us to test the hypothesis that miR-494 could target ATXN3 and subsequently downregulate HDAC3 and related histone acetylation to regulate neuronal death and plasticity in murine models of stroke.

Materials and methods

Clinical subjects

This study was approved by the Medical Ethics Committee of the Xuanwu Hospital of Capital Medical University, and was performed in accordance with the guidelines of the Declaration of Helsinki and Belmont Report. All subjects provided informed written consent prior to participation. This study was registered with ClinicalTrials.gov, number NCT03577093.

Patients with acute ischemic stroke (AIS) of the anterior circulation ($n = 76$) within 6 h after stroke symptom onset were included in this study. The patients underwent standard neurological and general medical evaluations and assessments with the National Institute of Health stroke scale (NIHSS) score at admission, and ischemic stroke was diagnosed in accordance with guidelines.[17] The inclusion criteria were as follows: (1) first ischemic stroke and admission within 6 h of symptom onset; (2) NIHSS score <25 points; (3) sudden occurrence of focal neurological deficits with exclusion of hemorrhage on computer tomography (CT); and (4) adequate access to patient information. The exclusion criteria included the following: (1) recurrent stroke; (2) hematologic diseases, malignant tumors, renal or liver failure; (3) history of mental disorders, severe dementia or coronary artery disease; and (4) other diseases affecting the hemogram. Age- and sex-matched healthy volunteers ($n = 52$) without any focal neurological deficit or history of central nervous system disease were recruited from the Medical Examination Center of Xuanwu Hospital. Some AIS patients were followed up for a year, and a modified Rankin rating score (mRS) was used to assess their prognosis.

Animals

All experimental protocols were approved by and conducted following rules and regulations of the Institutional Animal Care and Use Committee of Capital Medical University and reported according to the guidelines from ARRIVE (Animal Research: Reporting In Vivo Experiments). Male C57BL/6J mice weighing 20 to 22 g (two-month-old) were purchased from Vital River Laboratory Animal Technology Co., Ltd (Beijing, China), and were maintained in standard-housing open-top cages ($34 \times 16 \times 16$ cm) at a specific pathogen-free facility at 22–24°C with a relative humidity of 50–60% and on a 12 h:12 h light: dark cycle, with ad libitum access to water and standard laboratory chow diet at Xuanwu Hospital. Animal groups were randomized. Experimenters were blinded to the groups during surgery and other tests (behavior, neuroimaging and histology).

Middle cerebral artery occlusion and groups

Focal cerebral ischemia was induced by transient middle cerebral artery occlusion (MCAO).[18] Mice were anesthetized with 1.5% isoflurane in a 30% O_2/70% N_2O mixture and enflurane, and the right common carotid artery (CCA) was exposed. A nylon filament with a 0.19-mm diameter silicon tip was inserted to obstruct the flow of blood to the right MCA for a period of 45 min, after which it was

removed to allow for reperfusion. Body temperature was monitored and maintained at $37.0 \pm 0.5°C$ using a heating lamp during surgery. The dynamic changes of miR-494 in the ischemic brain tissue of MCAO mice were determined at 45 min after ischemia, one day, and three days after reperfusion by RT-PCR ($N = 6$ mice/group, total number = 24).

Mice were randomly divided into five groups with a lottery drawing box: (1) sham group: the mice underwent the same procedure as other groups without insertion of the suture; (2) MCAO + control group; (3) MCAO + miR-494 agomir group; (4) MCAO + miR-494 antagomir group; (5) MCAO + miR-494 antagomir + HDAC3 inhibitor RGFP966 (10 mg/kg) group. The mixture of miR-494 agomir, antagomir or control (100 μM, GenePharma, Shanghai, China) and Lipofectamine RNAiMAX Reagent was administered by right intracerebroventricular (ICV) injections immediately after MCAO as previously described.[19] The sequences were 5′-UGAAACAUACACGGGAAA CCUC-3′ (miR-494 agomir), 5′-GAGGUUUCCCGU GUAUGUUUCA-3′ (miR-494 antagomir), and 5′-CAGUACUUUU GUGUAGUACAA-3′ (control). Fluorochrome (FAM)-labeled miR-494 agomir was used to assess neural uptake after ICV delivery. RGFP966 was intraperitoneally injected immediately after reperfusion. Twelve mice from each group (total number = 60) were used to perform 2,3,5-triphenyl-2H-tetrazolium chloride (TTC)-staining at three days post-stroke. Moreover, six mice in each group (total number = 30) were used to perform Western blot (brain slices #1, 2) and immunofluorescence (brain slices #3–6) at three days post-stroke. In another set of experiments, 12 mice in each group (total number = 60) were used to detect regional cerebral blood flow until 14 days post-stroke. In addition, 12 mice in each group (total number = 60) were used to evaluate impaired fine motor and spatial learning and memory until 28 days post-stroke.

Primary cortical neuronal culture and groups

Embryonic brains were aseptically removed from wild-type (WT) mice.[20] Cortices from embryonic day 14 brains of C57BL/6J mice were dissected and suspended in Krebs buffer containing trypsin (Sigma-Aldrich, USA). After 15 min incubation at 37°C, fresh buffer with DNAse was added. The content was gently mixed and centrifuged at 1200 r/min for 3 min. The cell pellet was suspended in Neurobasal/B27/L-glutamine/Gentamicin medium, and viable cells were plated on culture plates precoated with poly-D-lysine at 200,000 cells/well. Seven-day-old cortical neurons were used for the experiments. Hypoxia was induced in neurons by incubation in a hypoxia chamber for 1 h or 6 h at an oxygen concentration of 1% in the presence of glucose. MiR-494 levels in primary neurons and supernatant after OGD were determined by RT-PCR ($N = 6$/group). In another set of experiments, neurons were transfected with control (20 nM), miR-494 agomir (20 nM), or miR-494 antagomir (20 nM). After two days of cultivation, the cells were collected to detect the levels of HDAC3 by real-time reverse transcription PCR (RT-PCR). Neurons were used to induce hypoxia by incubation in a hypoxia chamber for 1 h or 6 h at an oxygen concentration of 1% in the presence of glucose. The cells and supernatant were collected to detect the levels of miR-494 by RT-PCR. Neurons were divided into five groups: (1) control (20 nM), (2) control (20 nM) + 3 h OGD/ 24-h reperfusion, (3) miR-494 agomir (20 nM) + 3 h OGD/24-h reperfusion, (4) miR-494 antagomir (20 nM) + 3-h OGD/24-h reperfusion, and (5) miR-494 antagomir (20 nM) + 3-h OGD/ 24-h reperfusion + HDAC3 inhibitor RGFP966 (1 μM). Two days after transfection, OGD was performed, RGFP966 was added, and cells were cultivated for 24 h. Then, the neurons were assessed by lactate dehydrogenase (LDH) release, Western blot and high-content screening assays.

RT-PCR

Equivalent amounts of purified RNA from plasma, brain tissue, neurons and supernatant were used as a template to synthesize cDNA using oligo-d(T) primers and SuperScript III/RNaseOUT Enzyme Mix (Invitrogen, Carlsbad, CA, USA). For miR quantification, total RNA was purified using the RNeasy Mini Kit (Qiagen, Gaithersburg, MD, USA). MiR abundance was assessed by qRT-PCR using All-in-One miR qRT-PCR Reagent Kits. MiR-494 primers for human plasma were 5′-GGGAGGTTGTCCGTG TTGT-3′ and 5′-GTGCGTGTCGTGGAGTCG-3′. MiR-494 primers for mouse neurons were 5′-GGGA GGTTGTCCGTGTTGT-3′ and 5′-GTGCGTGTCG TGGAGTCG-3′. ATXN3 primers for mouse neurons were 5′-CCATCTTCCACGAGAAACAAG-3′ and 5′-TGTAAAA ATGTGCGGTAGTCTTC-3′. HDAC3 primers for mouse neurons were 5′-GTGGCTACA CTGT CCGAAATG-3′ and 5′- GTCATACGTCAG GAGGTCTGC-3′. Relative gene expression was calculated via the $2^{-\Delta\Delta CT}$ method, normalized, and expressed as fold change relative to U6 or β-actin.

Calculation of infarct volume and swelling

Experimental protocol for calculation of infarct volume and swelling, TUNEL/NeuN staining, immunofluorescence, and Western blotting is shown in Figure 2(a). Mice were sacrificed 72 h after reperfusion, and their

brains were quickly removed and processed for TTC staining and calculation of cerebral infarct volume. Ischemic lesions were traced in each slice in a blinded manner, and the total volume of infarction was calculated with correction for edema using ImageJ software. The infarct volume was calculated by subtracting the area of the noninfarcted area in the ischemic hemisphere from the area of the respective contralateral hemisphere. Volume calculation with edema correction was performed blindly using the following formula: swelling (% contralateral hemispheric volume) = (contralateral hemisphere volume − noninfarct ipsilateral hemisphere volume)/contralateral hemisphere volume × 100. In this experiment, there were 12 animals in each group, and the three-day survival rate was as follows: no animals died in the sham group (100%), two mice died in the MCAO group (83.3%), two mice died in the MCAO + microRNA-494 agomir group (83.3%), two mice died in the MCAO + microRNA-494 antagomir group (83.3%), and one mouse died in the MCAO + microRNA-494 antagomir + RGFP966 group (91.7%).

TUNEL/NeuN staining

The brain tissues were fixed in 4% paraformaldehyde for at least 48 h followed by dehydration in 30% sucrose. Coronal sections were sliced into 25-μm-thick sections using a cryostat vibratome for immunofluorescence as previously described. The frozen sections were blocked with 0.3% (w/v) bovine serum albumin (BSA) in PBS at room temperature for 1 h. Sections were incubated with primary antibodies against (Millipore, Bedord, USA) overnight at 4°C. After the sections were incubated with fluorescent-conjugated secondary IgG antibodies, they were counterstained with 4′,6-diamidino-2-phenylindole (DAPI). The images were digitized using an Olympus Fluoview FV1000 microscope (Olympus, Japan). The number of cells positive for NeuN/TUNEL staining was calculated and analyzed in the region of the ischemic peripheral cortex using ImageJ software.

Immunofluorescence

Immunohistochemistry was performed on 25-mm-thick coronal brain slices. The sections were incubated with the primary antibody against microtubule-associated protein (MAP)-2 (Cell Signaling Technology, MA, USA), HDAC3 (Abcam, CA, USA), and NeuN (Millipore, MD, USA) at 4°C overnight. Nonspecific antibody binding was blocked by incubation in 5% normal donkey serum (Jackson ImmunoResearch). After the sections were incubated with secondary antibodies conjugated with DyLight 488 or Cy3 (Jackson ImmunoResearch), they were counterstained with 4′,6-diamidino-2-phenylindole (DAPI). The images were digitized using an Olympus Fluoview FV1000 microscope (Olympus, Japan). The number of cells positive for NeuN/TUNEL staining was calculated and analyzed in the region of the ischemic peripheral cortex with ImageJ software.

Western blotting

The right hemisphere was dissected from MCAO and sham-operated mice. Brain tissue and cell samples were processed for Western blot analysis as previously described.[21] Primary antibodies used targeted the following: MAP-2, acetyl-histone H3 (Lys9/Lys14), histone 3, acetyl-histone H4 (Lys5), histone 4 (Cell Signaling Technology, MA, USA), HDAC3 (Abcam, CA, USA), and β-actin (Santa Cruz, CA, USA). Antigen-antibody complexes were observed by enhanced chemiluminescence using an Immobilon Western blotting kit. The intensity of the bands was detected using a FluorChem®HD2 Gel Imaging System (Protein Simple, USA). The gray value of bands was analyzed by AlphaEase FC software (Alpha Innotech, CA, USA).

Two-dimensional laser speckle imaging and blood pressure measurement

Regional cerebral blood flow (CBF) was monitored using the laser speckle imaging technique, and mean blood pressure (MBP) was recorded by tail cuff plethysmography using a physiological pressure transducer coupled to a data-acquisition system (ADInstruments, Australia). CBF and MBP were detected before ischemia, after the onset of ischemia (10 min after MCAO), after ischemia (45 min after MCAO), and after reperfusion (10 min, 1 day, 3 days, and 14 days after reperfusion). Changes in CBF were expressed as a percentage of pre-MCAO baseline values. MBP was measured by the same experimenter at approximately the same time of day at every time point. To facilitate vasodilatation, animals were placed in an insulated heat box at 35°C–36°C for 10 min. Five successive MBP readings at each session were recorded, and the average was calculated. The change in MBP between baseline and the day of MCAO was calculated for each mouse.

Behavioral testing and brain atrophy volume

Deficits in fine motor coordination were assessed with the balance beam test, and spatial learning and memory were examined using the Morris water maze.[22] In this experiment, there were 12 animals in each group, and the 28-day survival rate was as follows: no animals died

in the sham group (100%), three mice died in the MCAO group (75%), two mice died in the MCAO + microRNA-494 agomir group (83.3%), two mice died in the MCAO + microRNA-494 antagomir group (83.3%), and one mouse died in the MCAO + microRNA-494 antagomir + RGFP966 group (91.7%).

Beam balance test. Animals were trained for three days prior to injury on a beam/peg board walking motor function test.[23] On the 4th day before MCAO modeling, the mice were trained to learn the beam walking skill. Mice that could not pass the balance beam skillfully within 15 s were excluded. Beam walking tests were performed on the 1st, 3rd, 5th, 7th, 10th, 14th, 21st, and 28th days after MCAO according to the protocol requirements. Mouse were placed on a beam and scored based on the walking status of the mice with criteria as follows: 0 points, the mouse could not stay on the beam; 1 point, the mouse remained on the beam for 120 s but did not move; 2 points, the mouse moved on the beam but failed to pass the beam and dropped midway; 3 points, the mouse passed the beam successfully, but the affected hind leg showed more than 50% foot slips; 4 points, the mouse passed the beam successfully with more than one but less than 50% foot slips; 5 points, the mouse passed the beam successfully with only one foot slip; 6 points, the rat passed the beam without foot slips.

Morris water maze test. Briefly, mice were trained five times a day at 20-min intervals for each day for three consecutive days (25–27 days after MCAO). In each trial, mice were given 120 s to find the platform. Twenty-eight days after MCAO, a probe trial was performed with the platform removed, and the numbers of platform crossings and the percentage of time spent in the target quadrant were recorded. Swimming was video tracked, and latency, path length, swim speed, and cumulative distance from the platform were recorded. The mean swim latency for each day was evaluated and compared among groups. In the first three days after MCAO, neurological functions were evaluated by a six-point scale as follows: 0, no visible neurological deficits; 1, failure to extend right forepaw completely, suggesting mild focal neurological deficits; 2, circling to the right, suggesting moderate focal neurological deficits; 3, falling to the right, indicating severe focal neurological deficits; 4, no spontaneous walking and depressed level of consciousness; 5, unresponsive to stimulation or death due to brain ischemia.

Brain atrophy volume. The mice were sacrificed 14 days after transient MCAO. The atrophy area was measured using ImageJ software. The brain tissue loss area for each section was measured using the following equation: (volume of contralateral hemisphere – volume of ipsilateral hemisphere)/volume of contralateral hemisphere × 100%. The mean brain tissue loss volume was then determined by multiplying the mean loss area by the thickness of the evaluated tissue.

High-content screening assay

The 96-well plate was blocked with 0.3% (w/v) BSA in PBS at room temperature for 1 h (N = 6/group). The cells were incubated with primary antibodies against MAP-2 overnight at 4°C. After the plate was incubated with fluorescent-conjugated secondary IgG antibodies (Jackson Immunoresearch), all wells were counterstained with DAPI. Neurite outgrowth evaluation was observed under a phase-contrast microscope using a 10× objective of ImageXpress Micro XLS System (ImageXpress Micro XLS System, Molecular Devices, USA).

Statistical analysis

Statistical analysis was performed using SPSS 23.0 software. Numeric data are presented as the mean ± standard deviation. Student's *t* test was used for two-group comparisons. One-way ANOVA with Tukey–Kramer post hoc test was used for comparisons among several quantitative variables. The correlation between two variables was assessed using Pearson's correlation test. Data for neurobehavioral tests were analyzed by a two-way repeated measures (RM) ANOVA followed by the Bonferroni post hoc correction. $P < 0.05$ was considered statistically significant.

Results

MiR-494 was increased in the plasma of AIS patients and the MCAO mouse model

The clinical value of miR-494 for ischemic stroke is important to explore. Plasma samples were collected from 76 AIS patients within 6 h after cerebral ischemia and 52 controls, and miR-494 expression was significantly higher in AIS patients (Figure 1(a), $P < 0.01$). To assess whether miR-494 levels could predict functional outcome, we analyzed the relationship between plasma miR-494 levels within 6 h after ischemia and mRS a year after stroke. A significant positive correlation existed between plasma miR-494 levels and mRS at one year after symptom onset (Figure 1(b), $P < 0.01$). MiR-494 levels in the plasma of AIS patients with mRS ≥2 were significantly higher than in those with mRS <2 (Figure 1(c), $P < 0.05$). Therefore, high plasma miR-494 levels in patients with AIS are associated with
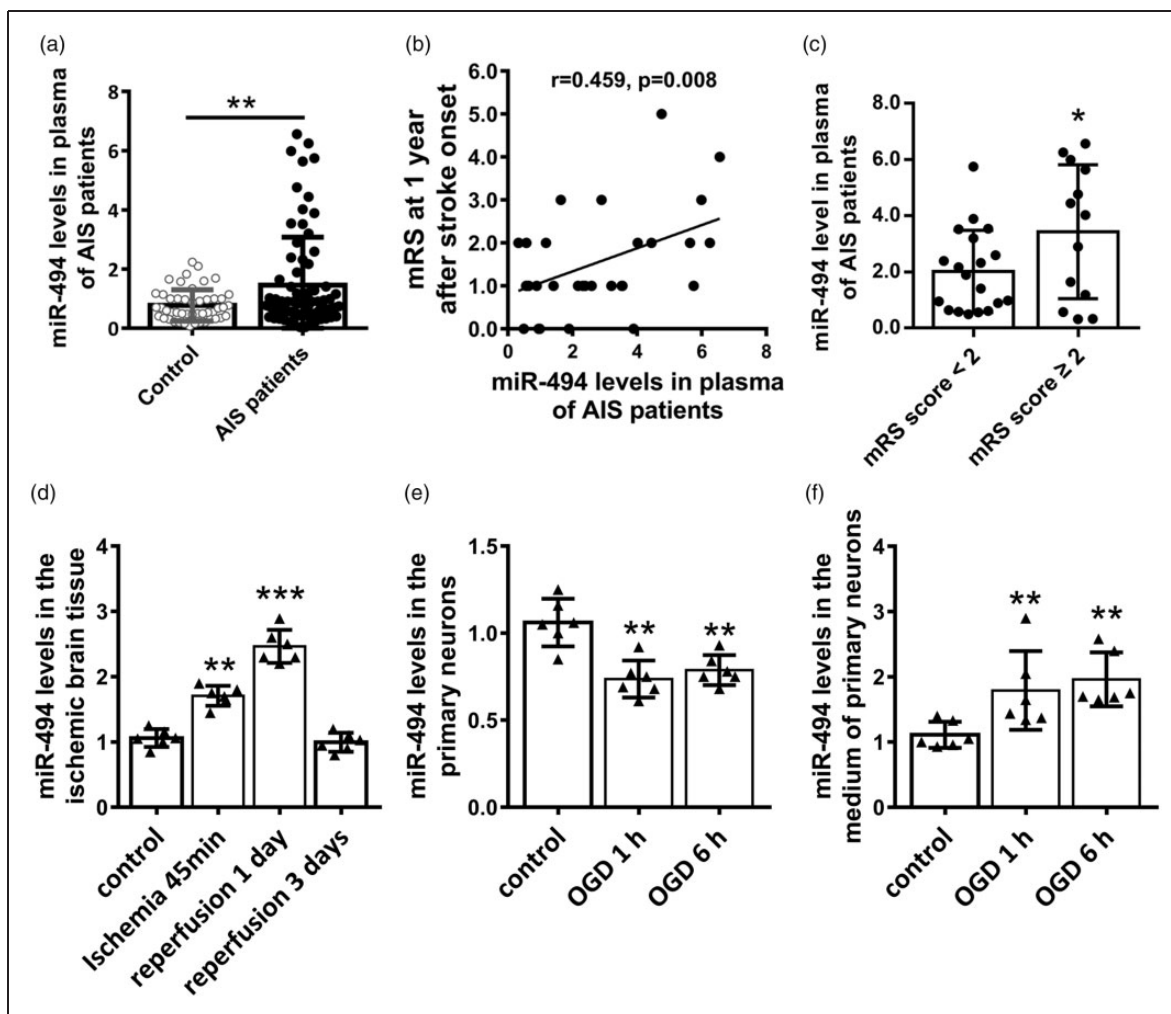
Figure 1. MiR-494 was increased in the plasma of AIS patients and the supernatant of primary neurons. (a) Expression of miR-494 in plasma of AIS patients ($n = 76$) and control volunteers ($n = 52$) was measured by RT-PCR. Student's t test. (b) Pearson correlation coefficient between plasma miR-494 level and mRS after one year. $n = 32$. (c) Comparison of miR-494 levels in the plasma of AIS patients with mRS ≥ 2 ($n = 13$) and patients with mRS < 2 ($n = 19$). Student's t test. (d) MiR-494 levels in the ipsilateral brain tissue of a mouse model of MCAO 45 min after ischemia and one day and three days after reperfusion. $n = 6$ per group. One-way ANOVA with Tukey–Kramer post hoc test. (e–f) MiR-494 levels in primary neurons and supernatant at different time points after OGD were determined by real-time PCR, with U6 used as an internal control. $n = 6$/group. One-way ANOVA with Tukey–Kramer post hoc test. *$P < 0.05$, **$P < 0.01$ vs. control group.

worse long-term functional outcomes. The dynamic changes of miR-494 in the ischemic brain tissue of mice were determined at 45 min after ischemia, one day, and three days after reperfusion. Compared with the expression in the sham group, the expression of miR-494 in the infarcted brain tissue of the MCAO group was significantly increased at 45 min after ischemia and 1 day after reperfusion (Figure 1(d), $P < 0.05$), and the expression returned to normal levels at three days after reperfusion. Furthermore, we detected miR-494 expression in the cortical primary neurons as well as the supernatant after OGD by RT-PCR. MiR-494 expression was significantly decreased at 1 h and 6 h

post OGD in neurons (Figure 1(e), $P < 0.05$) but increased at 1 h and 6 h post OGD in the supernatant (Figure 1(f), $P < 0.05$). Taken together, these results indicated that the upregulated miR-494 in plasma may be released from injured neurons.

MiR-494 protected against mouse cerebral I/R injury in the acute stage and the recovery stage

Because miR-494 expression was decreased in primary neurons, we evaluated the role of miR-494 in cerebral ischemic injury by giving mice miR-494 agomir via ICV injection immediately after MCAO. FAM-labeled
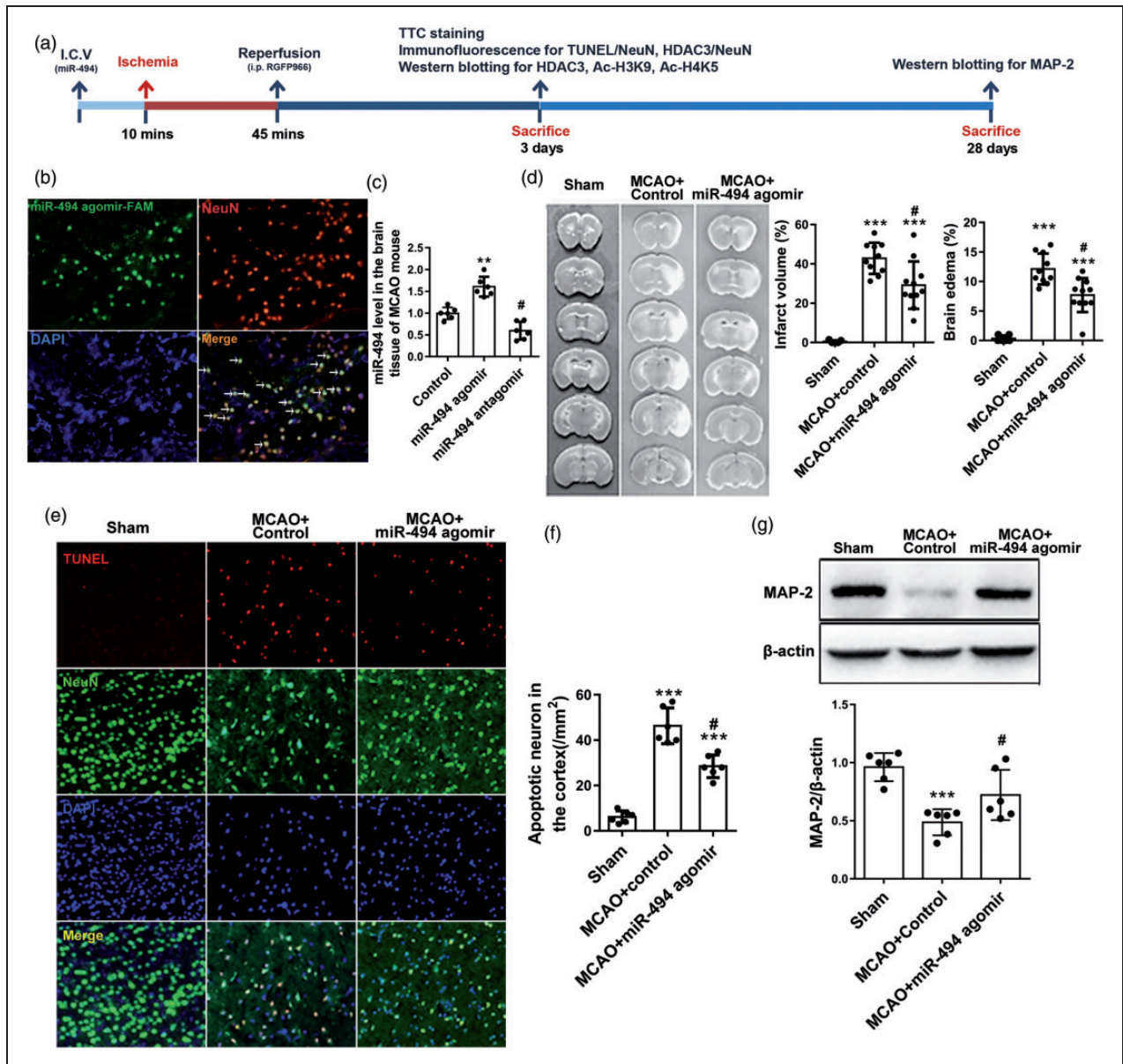
Figure 2. MiR-494 protected the brain against mouse ischemic injury in the acute stage and recovery stage. (a) Experimental protocol. (b) FAM-labeled miR-494 agomir with green fluorescence was used to assess neuronal uptake (red) after ICV delivery. Green fluorescence was mainly distributed in neurons (arrows) in the brain tissue. (c) QuantitativePCR was performed to verify the efficacy of miR-494 agomir and antagomir transfection. $n = 6$/group. (d) Cerebral infarct volume and brain edema evaluated by TTC staining of coronal brain sections. $n = 10–12$/group. (e–f) Neuronal apoptosis in the ipsilateral cortex as detected by TUNEL/NeuN immuno-fluorescence double staining. $n = 6$ per group. (g) Immunoblot of MAP-2 in the cortex in the recovery stage. $n = 6$/group. MCAO + control denotes mice subjected to 45 min ischemia followed by reperfusion for three days, with control administered by ICV injection immediately after ischemia; MCAO + miR-494 denotes mice subjected to 45 min ischemia followed by reperfusion for three days, with miR-494 agomir administered by ICV injection immediately after ischemia. $*P < 0.05$, $**P < 0.01$, $***P < 0.001$ vs. sham group. $\#P < 0.05$ vs. MCAO + control group. One-way ANOVA with Tukey–Kramer post hoc test.

miR-494 agomir was used to assess neural uptake after ICV delivery. Green fluorescence was mainly distributed in neurons in the brain tissue (Figure 2(b)). Quantitative PCR was performed to verify the efficacy of miR-494 agomir and antagomir transfection and

showed that miR-494 levels were upregulated after agomir injection and were downregulated after antagomir injection (Figure 2(c), $P < 0.05$). At 72 h after reperfusion, infarct volume, brain edema, and neuronal apoptosis were evaluated. TTC staining showed that no

infarction was observed in the sham group, and miR-494 agomir reduced cerebral infarct volume and brain edema relative to MCAO alone (Figure 2(d), $P < 0.05$). Thus, we calculated the apoptotic cell numbers in the cortex of the peri-infarction area. Few TUNEL-positive cells were detected in the sham-operated mice; in contrast, MCAO increased the number of TUNEL/NeuN-positive cells, which was abrogated by miR-494 agomir treatment (Figure 2(e) and (f), $P < 0.05$). In addition, MAP-2 immunoblotting demonstrated that miR-494 agomir significantly decreased neuronal injury at 28 days after reperfusion in the recovery stage (Figure 2(g), $P < 0.05$). These results demonstrated that miR-494 attenuates cerebral ischemic neuronal injury in the cortex.

MiR-494 downregulated HDAC3 expression in cortical neurons of MCAO mice

To investigate the effect of miR-494 on HDAC3 expression and the modulation of histone acetylation in vivo, HDAC3, acetyl-histone H3 (Lys9/Lys14)/histone 3 and acetyl-histone H4 (Lys5)/histone 4 expression in the ipsilateral cortex were assessed by Western blot. The HDAC3 protein level was significantly higher in the MCAO group than in the sham control, and this increase was downregulated by miR-494 agomir (Figure 3(a), $P < 0.05$). Meanwhile, histone acetylation of acetyl-H3K9 was significantly lower in the MCAO group than in the sham group, and this change was obviously reversed by miR-494 agomir (Figure 3(a),
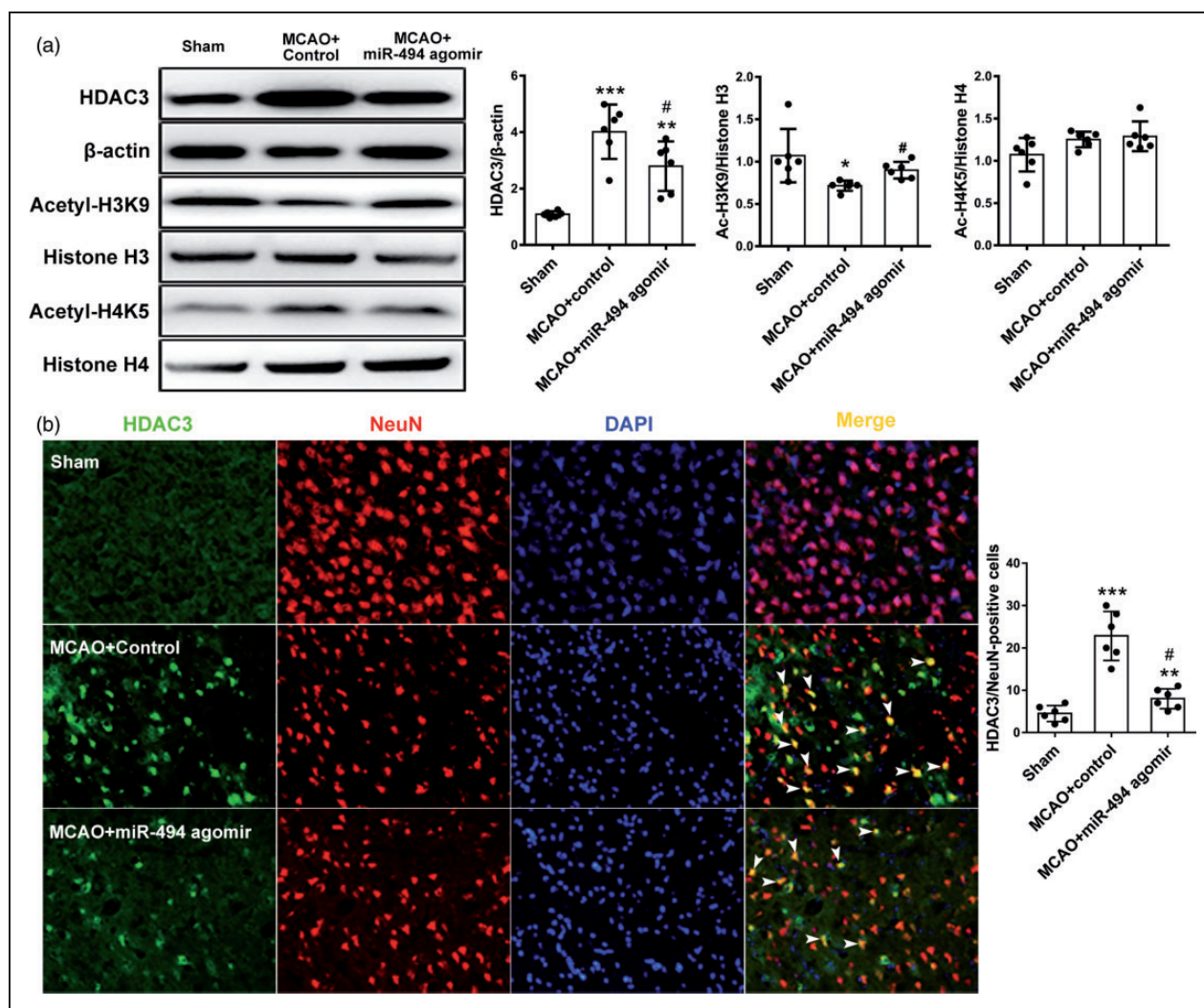
Figure 3. MiR-494 downregulated HDAC3 expression in neurons of MCAO mice. (a) Protein expression levels of HDAC3 and acetyl-histone H3 (Lys9/Lys14), histone 3 acetyl-histone H4 (Lys5), and histone 4 in the ipsilateral cortex were assessed by Western blot ($n = 6$/group). (b) The localization of HDAC3 in neurons was assessed by HDAC3/NeuN immunofluorescence double staining ($n = 6$/group). ***$P < 0.001$ vs. sham group; #$P < 0.05$ vs. MCAO + control group. One-way ANOVA with Tukey–Kramer post hoc test.

$P < 0.05$). However, acetyl-H4K5 expression was not changed significantly by MCAO or miR-494 agomir treatment (Figure 3(a)). To further determine the involvement of HDAC3 in the neuron, the localization of HDAC3 was assessed. Immunofluorescence showed that the miR-494 agomir reduced HDAC3 expression in neurons, as demonstrated by the decreased number of HDAC3/NeuN-positive cells (Figure 3(b), $P < 0.05$). These results proved that miR-494 attenuates HDAC3 expression and promotes acetyl-H3K9 levels in cerebral ischemic neurons in the ipsilateral cortex.

MiR-494 downregulated ATXN3 and HDAC3 in primary neurons

It has been proved that miR-494 downregulated ATXN3 through interacting with the 3′ UTR of ATXN3,[14] which positively regulates HDAC3 by deubiquitinating and stabilizing HDAC3.[15] In present context, to determine whether miR-494 target ATXN3 in cortical primary neurons, the changes of ATXN3 and HDAC3 expression were detected by RT-PCR after miR-494 intervention. The levels of ATXN3 and HDAC3 mRNA in the neurons were decreased by miR-494 agomir and were remarkably increased by miR-494 antagomir (Figure 4(a) and (b), $P < 0.05$). These in vitro tests confirmed that miR-494 directly targets HDAC3 in neurons. To assess the direct protective effects of miR-494 on neurons, we transfected primary cortical neurons with miR-494 agomir or control and exposed them to OGD. Concomitant with the in vivo data, the OGD exposure-induced increase in LDH release was reversed by miR-494 agomir treatment (Figure 4(c), $P < 0.05$). To investigate the effects of miR-494 on axon injury, we examined MAP-2 content by Western blot. MAP-2 expression in primary cortical neurons, which was reduced upon exposure to OGD, was elevated by miR-494 agomir treatment (Figure 4(d), $P < 0.05$). Additionally, the reduction in axon injury elicited by OGD/R plus miR-494 antagomir was blocked by HDAC3 inhibitor RGFP966 treatment (Figure 4(e), $P < 0.05$). These results suggested that miR-494 targets ATXN3 in cortical primary neurons and inhibits the expression of HDAC3, and positively upregulates the expression of the axon protein MAP-2 by HDAC3 inhibition, thereby suppressing OGD-induced axon injury in primary cortical neurons.

HDAC3 inhibition reversed miR-494 antagomir-aggravated acute cerebral ischemic injury

To investigate whether miR-494 antagomir promotes ischemic brain injury in MCAO mice via upregulation of HDAC3, RGFP966 was injected intraperitoneally immediately following reperfusion, and infarct volume and brain edema of MCAO mice were detected at three days post reperfusion. We found that the downregulated acetyl-H3K9 levels in the ischemic brain cortex after miR-494 antagomir treatment were reversed by the HDAC3 inhibitor (Figure 5(a), $P < 0.05$). Consistently, RGFP966 also reversed miR-494 antagomir-aggravated cerebral brain injury (Figure 5(b), $P < 0.05$). These in vivo results demonstrated that miR-494 attenuates cerebral ischemic injury in the acute stage by targeting HDAC3.

HDAC3 inhibition reversed the miR-494 antagomir-worsened long-term outcome

Whether miR-494 agomir treatment would improve the long-term outcomes of mouse stroke by targeting HDAC3 was further investigated. Motor function recovery and learning and memory ability were detected by the balance beam test and Morris water maze, respectively, and brain atrophy was calculated in mice at 28 days after MCAO. The atrophic brain volume of mice at 28 days post reperfusion was significantly reduced by miR-494 agomir treatment (Figure 6(a), $P < 0.05$). RGFP966 also significantly reduced the atrophic brain volume of mice (Figure 6(a), $P < 0.05$). As blood flow might also be affected by the miR-494 agomir or antagomir, CBF was monitored during ischemia and reperfusion. There were no significant differences among the four groups in preischemic CBF baseline values or in CBF changes at 10 min after ischemia or 10 min, 1 day, 3 days, or 14 days after reperfusion (Figure 6(b)). In addition, there were no significant differences among the four groups in preischemic MBP baseline values or in MBP changes at 10 min after ischemia or 10 min, 1 day, 3 days, or 14 days after reperfusion (Figure 6(c)). The balance beam test at 1, 3, 5, 7, 10, 14, 21, and 28 days after reperfusion showed that the miR-494 agomir significantly improved motor function in mice after cerebral ischemic injury (Figure 6(d), $P < 0.05$). In contrast, miR-494 antagomir further strengthened neurological deficiency but not significantly. The HDAC3 inhibitor significantly improved the motor function recovery of mice with miR-494 antagomir treatment (Figure 6(e), $P < 0.05$). The Morris water maze at 28 days post reperfusion showed that the escape latency of mice was significantly shortened by miR-494 agomir treatment (Figure 6(f) and (g), $P < 0.05$); in contrast, miR-494 antagomir treatment further strengthened the memory impairment but not significantly. The HDAC3 inhibitor significantly shortened the escape latency of mice (Figure 6(f) and (g), $P < 0.05$). These data suggested that the miR-494 agomir improves long-term outcomes of mouse stroke by targeting HDAC3.
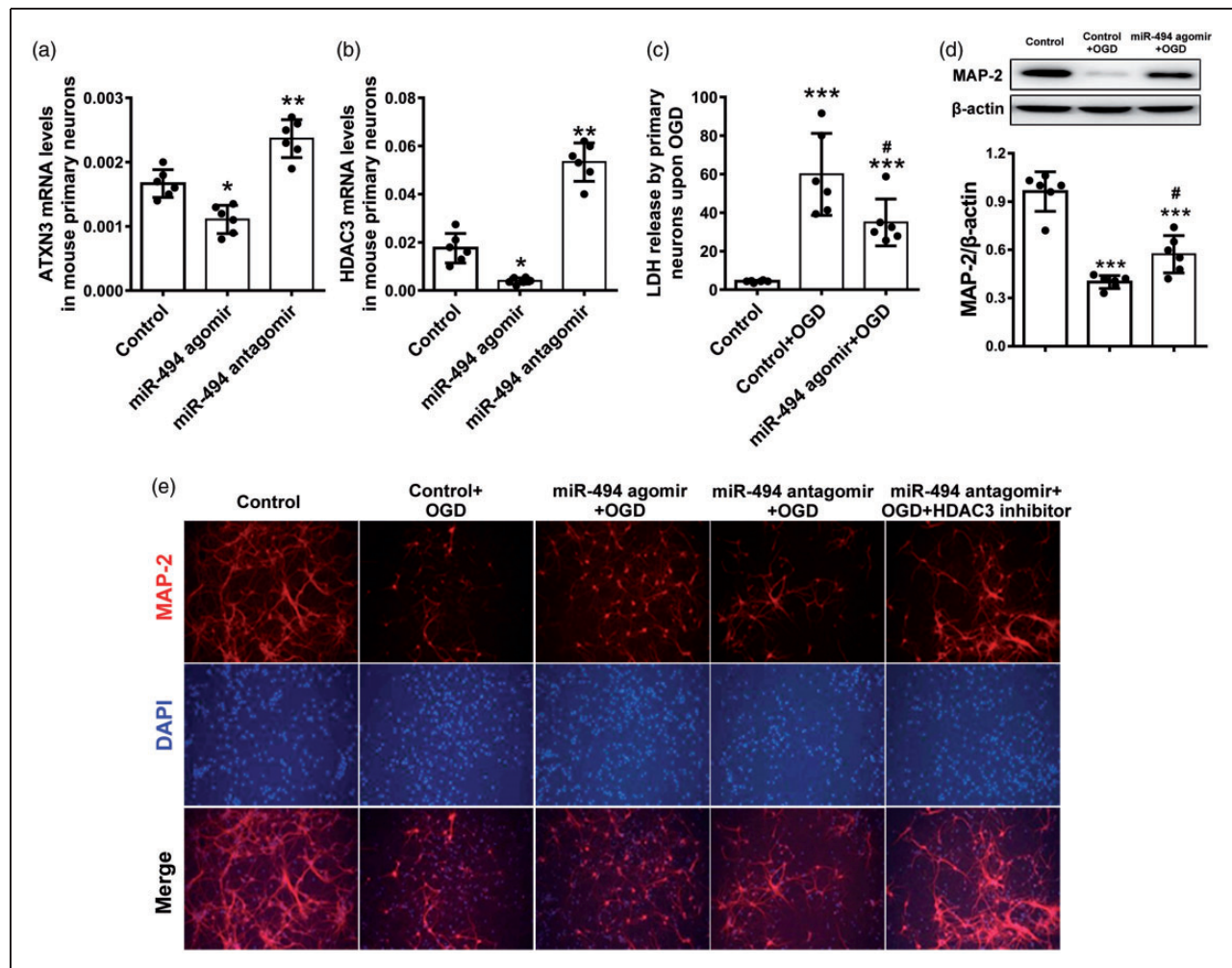
Figure 4. MiR-494 downregulated HDAC3 in cortical primary neurons. (a–b) Expression of ATXN3 and HDAC3 in mouse primary neurons was measured by RT-PCR following transfection with miR-494 agomir or antagomir ($n = 6$/group) for 48 h. (c) LDH release in neurons transfected with miR-494 agomir for 48 h and then exposed to OGD/R for 2 h/24 h ($n = 6$/group). (d) MAP-2 expression in neurons transfected with miR-494 agomir for 48 h and then exposed to OGD/R 2 h/ 24 h was detected by Western blot ($n = 6$/group). (e) MAP-2 expression in neurons following OGD was detected by immunofluorescence ($n = 6$/group). Neurons were transfected with control, miR-494 agomir, or miR-494 antagomir for 48 h and then exposed to OGD/R 2 h/24 h, with the addition of RGFP966 at the time of reoxygenation. OGD/R: oxygen and glucose deprivation/reoxygenation. *$P < 0.05$, **$P < 0.01$ vs. control group. #$P < 0.05$ vs. control + OGD group. One-way ANOVA with Tukey–Kramer post hoc test.

Discussion

The present findings show that epigenetic mechanisms may feasibly control neural plasticity and memory formation following ischemic stroke. We showed that plasma miR-494 levels were significantly higher in AIS patients than in matched controls and were associated with worse long-term prognosis. In experimental stroke, the expression of miR-494 in the infarcted brain tissue of MCAO mice was transiently increased after ischemia. In vitro, miR-494 levels were decreased in cortical primary neurons after OGD but were increased post OGD in the supernatant. Moreover, intracerebro-ventricular injection of miR-494 agomir reduced

cerebral ischemic injury in a mouse model. Mechanistically, miR-494 suppresses ATXN3 and HDAC3 expression, upregulates histone acetylation of acetyl-H3K9 in vivo and targets HDAC3 in primary neurons. HDAC3 inhibition reversed miR-494 antagomir-aggravated neuronal injury as well as acute cerebral ischemic injury and the long-term functional outcome deficiency. We reveal a novel function by which miR-494 targets HDAC3 to positively regulate a subset of neuronal genes via upregulation of acetyl-H3K9.

Currently, there are no blood-based biomarkers with clinical utility for functional outcome prediction of AIS patients. MiRNAs show promise as disease markers
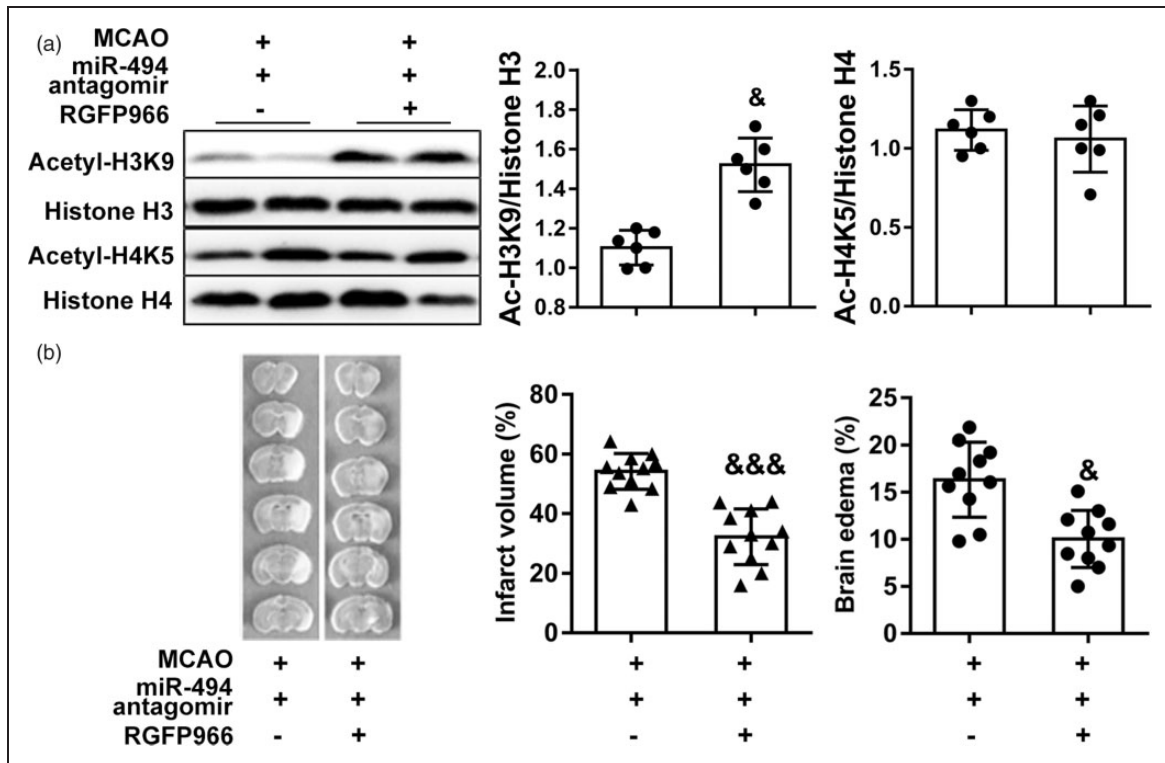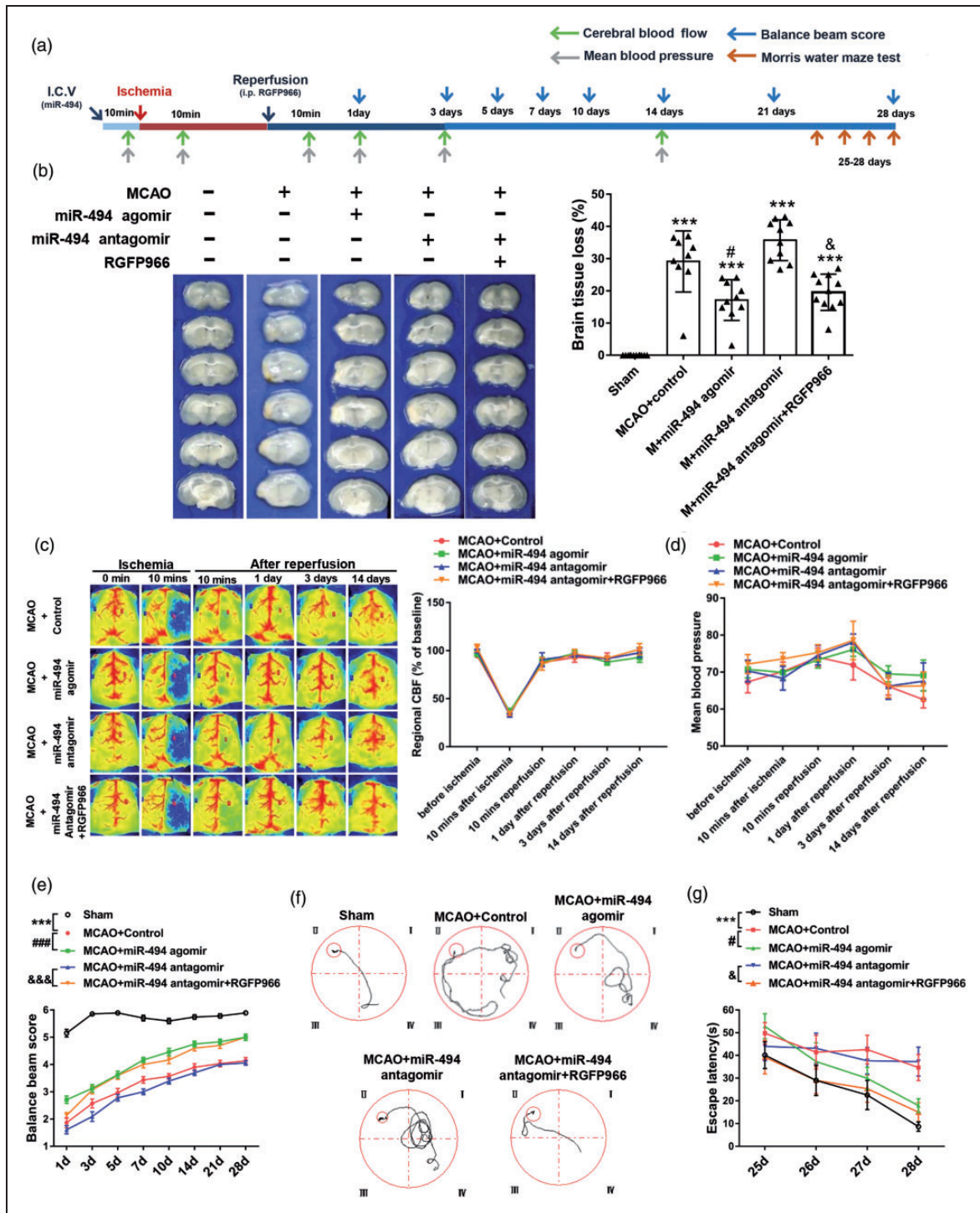
Figure 5. HDAC3 inhibition reversed miR-494 antagomir-aggravated acute cerebral ischemic injury. Mice were subjected to 45 min ischemia followed by reperfusion for three days, with miR-494 antagomir administered by ICV injection immediately after ischemia and RGFP966 injected intraperitoneally immediately following reperfusion. (a) Expression levels of HDAC3, acetyl-histone H3 (Lys9/Lys14), histone 3 acetyl-histone H4 (Lys5), and histone 4 in the ipsilateral cortex were assessed by Western blot. $n = 6$/group. (b) Cerebral infarct volume and brain edema evaluated by TTC staining of coronal brain sections. $n = 10–11$/group. [&]$P < 0.05$, [&&&]$P < 0.001$ vs. MCAO+ miR-494 antagomir group. Student's t test.

because of their cell type-specific expression patterns and stability in peripheral blood.[24] In our human study, we showed that miR-494 was increased in plasma following ischemic stroke compared with that in matched controls. In addition, miR-494 levels in the plasma of AIS patients with mRS ≥ 2 were significantly higher than those in the plasma of patients with mRS < 2, indicating that high plasma miR-494 levels are associated with poor long-term prognosis. Therefore, miR-494 may serve as an objective molecular tool to assess AIS severity and prognosis. We detected the expression of miR-494 in animal brains at different time points and found that its expression was transiently increased, suggesting that its elevation mainly plays a role in the acute brain injury process. In vitro, miR-494 levels were decreased in the cortical primary neurons after OGD but were increased in the supernatant post OGD, suggesting that plasma miR-494 might originate from injured neurons in the ischemic brain tissue. Accordingly, intracerebroventricular injections of miR-494 agomir reduced cerebral infarct volume, neuronal death and axon injury in vivo. There was no significant difference among the four

groups in preischemic CBF and MBP baseline values or CBF and MBP changes at 10 min after ischemia and reperfusion, suggesting that miR-494 directly affects neurons, rather than mediating neuroprotective effects by affecting CBF or MBP. Recently, miRNA treatment has been moved to clinical evaluation stages in some diseases. These clinical and basic research results demonstrate that miR-494 may be an attractive therapeutic target for the treatment of AIS.

Cognitive impairment is frequent after stroke. A major finding of this report is that a powerful negative regulator of memory formation, HDAC3, as a potential target of miR-494, is reduced in brain tissue after cerebral ischemia via a transcriptionally dependent pathway. MiR-193b-3p was recently reported to regulate chondrogenesis and chondrocyte metabolism by targeting HDAC3.[25] However, for the first time, our studies demonstrated downregulated mRNA expression of ATXN3 and HDAC3 in neurons, respectively. Since previous study has demonstrated that ATXN3 is the target gene of miRNA-494 by luciferase reporter gene experiment,[14] so we did not repeat this experiment. Hence, in the context of ischemic stroke,

Figure 6. HDAC3 inhibition reversed the miR-494 antagomir-worsened long-term outcome. (a) Experimental protocol. Mice were subjected to 45 min ischemia followed by reperfusion for 28 days, with control, miR-494 agomir, or miR-494 antagomir administered by ICV injection immediately after ischemia and RGFP966 injected intraperitoneally immediately following reperfusion. (b) Brain tissue loss at 28 days following stroke was calculated. One-way ANOVA with Tukey–Kramer post hoc test. (c) Regional CBF was monitored using two-dimensional laser speckle imaging techniques. Representative images and quantification of CBF before, during, and after transient MCAO. (d) MBP was recorded by tail cuff plethysmography using a physiological pressure transducer coupled to a data-acquisition system. (e) Motor function recovery was detected by the balance beam test. (f) Computer printouts of superimposed swimming trajectories of mice trained in light to find an invisible platform after starting in any of the four cardinal points (north, east, south, west) at the circumference of the pool. (g) Learning and memory ability were detected by escape latency in the Morris water maze. $n = 9$–12/group. Two-way RM ANOVA followed by the Bonferroni post hoc correction. $*P < 0.05$, $***P < 0.001$ vs. sham group; $^{\#}P < 0.05$ vs. MCAO + control group; $^{\&}P < 0.05$ vs. MCAO + miR-494 antagomir group.

miR-494 attenuates neuronal death, axon injury and long-term neurological function recovery. Attenuated recruitment of HDAC3 to promoter regions has been shown to potentiate the transcriptional initiation of genes including Hspa1a, Bcl2l1, and Prdx2, which may underlie the mechanism of protection of ischemic postconditioning.[4] Even though the neuroprotective function of miR-494 was similar to that of the HDAC3 inhibitor, their method of HDAC3 inhibition was different: the HDAC3 inhibitor RGFP966 reduced HDAC3 nuclear distribution in rat cortical neurons,[4] and miR-494 decreased HDAC3 expression but not nuclear localization in neurons. However, both reduced the level of histone H3 acetylation but not histone H4 acetylation, thereby alleviating neuron damage under hypoxic conditions. Overall, our data suggest that miR-494 may serve as a predictive biomarker of functional outcome in AIS patients and protect against ischemic injury by reducing neuronal apoptosis via inhibiting HDAC3.

However, some caveats exist. Although miR-494 antagomir upregulated HDAC3 expression in neurons in vitro, no significant increase in neuronal injury or infarct volume was observed in miR-494 antagomir-treated mice, suggesting that parallel compensatory signals may exist. Therefore, future studies will determine whether miR-494 targets astrocytes or microglia in addition to directly influencing neuronal cell death. MiR-494 likely has other targets in stroke beyond HDAC3, such as other proven targets including matrix metalloproteinase-9 (MMP-9),[26] PTEN/Akt,[27] cell cycle regulator p27,[28] and DNA damage repair-related RAD23B,[29] all of which are involved in cerebral ischemic brain injury. Further mechanistic studies are warranted to carefully dissect the complex pathways for miR-494 in stroke and neuronal death.

In summary, we showed, for the first time, that miR-494 may serve as an objective molecular tool to assess disease severity and prognosis of AIS. The identification of miRNAs as endogenous modulators of HDAC3 expression provides an alternative approach to target this protein and opens new perspectives for therapeutic applications. Our results indicate that the endogenous protective mechanism of miR-494 against brain injury is at least partly mediated by reducing neuronal death and axon injury via decreasing HDAC3 expression in neurons. We demonstrate that stroke may be treated with miR-494 agomir to amplify neural plasticity and enhance functional recovery. In this study, we used ICV injection to deliver miR-494 agomir, which is commonly used in basic research. It was previously thought that this method probably will not translate to clinical stroke therapies. But recent clinical trials have proved that thrombectomy has brought about significant benefits for acute ischemic stroke patients up to 24 h since

symptom onset.[30,31] Based on that, combination therapy of recanalization via endovascular thrombectomy and miR-494-based drugs might provide new insight for the treatment of ischemic stroke in the future.[32]

Declaration of conflicting interests

The author(s) declared no potential conflicts of interest with respect to the research, authorship, and/or publication of this article.

Authors' contributions

HZ, GL, SZ, FL, ZT, RW, QM, FY, JF, ZH, and LL performed the experimental components of the study, including cell culture, RT-PCR, immunofluorescence, immunoblot, and high-content screening assays. GL performed the MCAO animal surgery. HZ and GL analyzed and interpreted the data from behavioral tests, including performing statistical analysis. HZ and GL designed the study and wrote the manuscript. XJ and YL supervised the project. All authors read and approved the final manuscript.

ORCID iD

Yumin Luo https://orcid.org/0000-0002-2712-8974

References

1. Nott A, Cheng J, Gao F, et al. Histone deacetylase 3 associates with MeCP2 to regulate FOXO and social behavior. *Nat Neurosci* 2016; 19: 1497–1505.
2. Kwapis JL, Alaghband Y, Lopez AJ, et al. Context and auditory fear are differentially regulated by HDAC3 activity in the lateral and basal subnuclei of the amygdala. *Neuropsychopharmacology* 2017; 42: 1284–1294.
3. Alaghband Y, Kwapis JL, Lopez AJ, et al. Distinct roles for the deacetylase domain of HDAC3 in the hippocampus and medial prefrontal cortex in the formation and extinction of memory. *Neurobiol Learn Mem* 2017; 145: 94–104.
4. Yang X, Wu Q, Zhang L, et al. Inhibition of histone deacetylase 3 (HDAC3) mediates ischemic preconditioning and protects cortical neurons against ischemia in rats. *Front Mol Neurosci* 2016; 9: 131.
5. Pardo M, Cheng Y, Velmeshev D, et al. Intranasal siRNA administration reveals IGF2 deficiency contributes to impaired cognition in Fragile X syndrome mice. *JCI Insight* 2017; 2: e91782.
6. Kuboyama T, Wahane S, Huang Y, et al. HDAC3 inhibition ameliorates spinal cord injury by immunomodulation. *Sci Rep* 2017; 7: 8641.

7. Xia M, Zhao Q, Zhang H, et al. Proteomic analysis of HDAC3 selective inhibitor in the regulation of inflammatory response of primary microglia. *Neural Plast* 2017; 2017: 6237351.

8. Olaru AV, Ghiaur G, Yamanaka S, et al. MicroRNA down-regulated in human cholangiocarcinoma control cell cycle through multiple targets involved in the G1/S checkpoint. *Hepatology* 2011; 54: 2089–2098.

9. Arribas AJ, Campos-Martin Y, Gomez-Abad C, et al. Nodal marginal zone lymphoma: gene expression and miRNA profiling identify diagnostic markers and potential therapeutic targets. *Blood* 2012; 119: e9–e21.

10. Wang X, Zhang X, Ren XP, et al. MicroRNA-494 targeting both proapoptotic and antiapoptotic proteins protects against ischemia/reperfusion-induced cardiac injury. *Circulation* 2010; 122: 1308–1318.

11. Xiong R, Wang Z, Zhao Z, et al. MicroRNA-494 reduces DJ-1 expression and exacerbates neurodegeneration. *Neurobiol Aging* 2014; 35: 705–714.

12. Zhu H, Xie R, Liu X, et al. MicroRNA-494 improves functional recovery and inhibits apoptosis by modulating PTEN/AKT/mTOR pathway in rats after spinal cord injury. *Biomed Pharmacother* 2017; 92: 879–887.

13. Song S, Lin F, Zhu P, et al. Extract of Spatholobus suberctus Dunn ameliorates ischemia-induced injury by targeting miR-494. *PLoS One* 2017; 12: e0184348.

14. Carmona V, Cunha-Santos J, Onofre I, et al. Unravelling endogenous microrna system dysfunction as a new pathophysiological mechanism in Machado-Joseph Disease. *Mol Ther* 2017; 25: 1038–1055.

15. Feng Q, Miao Y, Ge J, et al. ATXN3 positively regulates Type I IFN antiviral response by deubiquitinating and stabilizing HDAC3. *J Immunol* 2018; 201: 675–687.

16. Teppen TL, Krishnan HR, Zhang H, et al. The potential role of amygdaloid microrna-494 in alcohol-induced anxiolysis. *Biol Psychiatry* 2016; 80: 711–719.

17. Prabhakaran S, Ruff I and Bernstein RA. Acute stroke intervention: a systematic review. *JAMA* 2015; 313: 1451–1462.

18. Hata R, Mies G, Wiessner C, et al. A reproducible model of middle cerebral artery occlusion in mice: hemodynamic, biochemical, and magnetic resonance imaging. *J Cereb Blood Flow Metab* 1998; 18: 367–375.

19. Zhao H, Wang J, Gao L, et al. MiRNA-424 protects against permanent focal cerebral ischemia injury in mice involving suppressing microglia activation. *Stroke* 2013; 44: 1706–1713.

20. Nichols M, Elustondo PA, Warford J, et al. Global ablation of the mitochondrial calcium uniporter increases glycolysis in cortical neurons subjected to energetic stressors. *J Cereb Blood Flow Metab* 2017; 37: 3027–3041.

21. Takagi T, Imai T, Mishiro K, et al. Cilostazol ameliorates collagenase-induced cerebral hemorrhage by protecting the blood-brain barrier. *J Cereb Blood Flow Metab* 2017; 37: 123–139.

22. Liu DZ, Waldau B, Ander BP, et al. Inhibition of Src family kinases improves cognitive function after intraventricular hemorrhage or intraventricular thrombin. *J Cereb Blood Flow Metab* 2017; 37: 2359–2367.

23. Brabazon F, Wilson CM, Jaiswal S, et al. Intranasal insulin treatment of an experimental model of moderate traumatic brain injury. *J Cereb Blood Flow Metab* 2017; 37: 3203–3218.

24. Tiedt S, Prestel M, Malik R, et al. RNA-Seq identifies circulating mir-125a-5p, mir-125b-5p, and mir-143-3p as potential biomarkers for acute ischemic stroke. *Circ Res* 2017; 121: 970–980.

25. Meng F, Li Z, Zhang Z, et al. MicroRNA-193b-3p regulates chondrogenesis and chondrocyte metabolism by targeting HDAC3. *Theranostics* 2018; 8: 2862–2883.

26. Sun T, Cheung KSC, Liu ZL, et al. Matrix metallopeptidase 9 targeted by hsa-miR-494 promotes silybin-inhibited osteosarcoma. *Mol Carcinog* 2018; 57: 262–271.

27. Chen HH, Huang WT, Yang LW, et al. The PTEN-AKT-mTOR/RICTOR pathway in nasal natural killer cell lymphoma is activated by mir-494-3p via PTEN but inhibited by mir-142-3p via RICTOR. *Am J Pathol* 2015; 185: 1487–1499.

28. Pollutri D, Patrizi C, Marinelli S, et al. The epigenetically regulated miR-494 associates with stem-cell phenotype and induces sorafenib resistance in hepatocellular carcinoma. *Cell Death Dis* 2018; 9: 4.

29. Comegna M, Succoio M, Napolitano M, et al. Identification of miR-494 direct targets involved in senescence of human diploid fibroblasts. *FASEB J* 2014; 28: 3720–3733.

30. Nogueira RG, Jadhav AP, Haussen DC, et al. Thrombectomy 6 to 24 hours after stroke with a mismatch between deficit and infarct. *N Engl J Med* 2018; 378: 11–21.

31. Bhaskar S, Stanwell P, Cordato D, et al. Reperfusion therapy in acute ischemic stroke: dawn of a new era? *BMC Neurol* 2018; 18: 8.

32. Sun P, Liu DZ, Jickling GC, et al. MicroRNA-based therapeutics in central nervous system injuries. *J Cereb Blood Flow Metab* 2018; 38: 1125–1148.